Electrocatalysis (2015) 6:117–125
DOI 10.1007/s12678-014-0229-7

Non-precious Metal Oxygen Reduction Nanocomposite Electrocatalysts Based on Poly(phenylenediamines) with Cobalt

Ya. I. Kurys · O. O. Ustavytska · V. G. Koshechko · V. D. Pokhodenko

Published online: 21 September 2014

Abstract The unpyrolyzed non-precious metal-polymer nanocomposite electrocatalysts for the oxygen reduction reaction (ORR) based on amino-substituted analogues of polyaniline (poly-*o*-phenylenediamine—PoPDA, poly-*m*-phenylenediamine—PmPDA), cobalt and carbon black were obtained. Composition, morphology, structure and electrochemical properties of nanocomposite electrocatalysts were characterized by C,H,N-analysis, atomic absorption spectrometry, scanning electron microscopy, powder X-ray diffraction, FTIR spectroscopy and cyclic voltammetry. It was shown that differences in the structure of PoPDA and PmPDA caused by the position of the amino groups in the aromatic ring of the starting monomers, as well as conditions for their preparation, are responsible for the difference in the electrochemical properties of hybrid composites based on such polymers. It was found that nanocomposite electrocatalysts based on PmPDA (ORR onset potential, E_{onset} up to 530 mV; ORR peak potential, E_p up to 325 mV vs. reversible hydrogen electrode, RHE) were more active in 0.05 M H_2SO_4, compared with the analogue based on PoPDA. Moreover, the activity of PmPDA- or PoPDA-based metal-polymeric composites for the ORR was higher than that for previously reported similar polyaniline-based composite, which may be due to effective formation and/or increase the number of active sites for the ORR in electrocatalysts at the expense of the presence of additional nitrogen atoms in poly(phenylenediamines).

Keywords Oxygen reduction reaction · Unpyrolyzed non-precious metal electrocatalysts · Poly(phenylenediamines) · Cobalt

Y. I. Kurys (✉) · O. O. Ustavytska · V. G. Koshechko · V. D. Pokhodenko
L.V. Pysarzhevsky Institute of Physical Chemistry of the NAS of Ukraine, 31 Nauky Pr., Kyiv 03028, Ukraine
e-mail: kurys@inphyschem-nas.kiev.ua

Introduction

Replacement of platinum in electrocatalysts for oxygen reduction reaction (ORR) is an essential problem associated with the commercialization of low temperature fuel cells, particularly with solid polymer electrolyte [1, 2]. The carbon-supported catalysts, obtained by pyrolysis (500–900 °C) of nitrogen-containing macrocyclic complexes of Co and Fe (porphyrins, phthalocyanines, etc.) were among the first precious metal-free ORR electrocatalysts, capable to exhibit high activity and stability in an acidic medium or in acidic environment of the cathode (when using a solid polymer electrolyte) [2–4]. This approach was used later to prepare so called Me–N–C catalysts by pyrolysis of cheaper (compared to the nitrogen-containing macrocycles) starting compounds—various nitrogen-containing precursors (ammonia, acetonitrile, polyacrylonitrile, amines, etc.), different salts of Co and Fe as well as different kinds of carbon component [2, 4–6].

In recent years, significant progress in creation of various non-precious metal ORR electrocatalysts was achieved, and such systems as W carbides with addition of Ta or Cr; carbon-supported Mo and W nitrides; Zr oxynitride and Fe carbonitride; and Co and Co–Ni sulfides [4], a number of N-doped nanoscale carbon materials (carbon nanotubes [7] and graphene [8]), and others were reported. However, only some of Me–N–C catalysts obtained by simultaneous pyrolysis of the corresponding carbon, nitrogen and transition metal precursors were evaluated [4] as a possible real alternative to Pt.

It is known [9–12] that conducting organic polymers (CPs) like polyaniline (PANI), polypyrrole (PPy), polythiophene, etc., as well as composites based thereon, can be used as ORR electrocatalysts. Besides that, high-performance Me–N–C ORR catalysts were obtained by pyrolysis of nitrogen-containing CPs, transition metals (Co, Fe or a combination thereon) and carbon materials [2, 4, 13–17]. Recently, it was proposed to use unpyrolyzed carbon-supported metal-

polymer ORR electrocatalysts based on CPs and cobalt [13, 18–23], which to certain extent can be considered as mimetics of Co-containing porphyrins. The main feature of metal-polymer electrocatalysts is their sufficiently higher ORR activity and stability in acidic electrolyte without additional thermal treatment that distinguishes them from other known Me–N–C systems.

Only PPy or PANI as a components of unpyrolyzed metal-polymer electrocatalysts based on nitrogen-containing CPs were reported in literature. At the same time, the use of, for example, amino-substituted analogues of the PANI—poly(*o*-, *m*- or *p*-)phenylenediamines in such composite electrocatalysts may lead to formation of additional C/MeN_x sites, on which activation and catalytic conversion of O_2 occur [2, 4–6]. It can be supposed that metal-polymer composites based on poly(*o*-phenylenediamine) (PoPDA) or poly(*m*-phenylenediamine) (PmPDA) with cobalt or iron have high potential to be used as ORR electrocatalysts due to high quantity of unsaturated nitrogen atoms (which is higher than in PPy or PANI per formula unit), and the fragments of their structure to a certain extent similar to porphyrins or phthalocyanines. It was shown [24] that PoPDA can be used as polymeric donor of nitrogen for formation of sufficiently efficient Co or Fe–N/C catalysts for ORR by pyrolysis. Surprisingly, the information about such unpyrolyzed composites, to the best of our knowledge, is absent in the literature. In our opinion, such electrocatalysts may be an alternative, at least, to analogues based on PANI. Moreover, the differences between structure of PoPDA and PmPDA may lead to differences of electrochemical characteristics of composites based on them.

Given the above, the aim of the work was to obtain metal-polymer nanocomposite electrocatalysts for ORR based on *o*- and *m*-substituted analogues of PANI (PoPDA, PmPDA), cobalt and carbon black, and to study the effects of (i) conditions for such systems preparation and (ii) the differences in the molecular structure of the polymer components, caused by the position of the amino groups in aromatic ring, on the composition, structure and electrochemical properties of the nanocomposites.

Experimental

Synthesis of Composites

o-Phenylenediamine (Aldrich, 99.5 %) and *m*-phenylenediamine (Acros Organics, 99+%), highly dispersed acetylene black with a bulk density of 80–120 g/l (Alfa Aesar, 99.9+%), $Co(NO_3)_2 \times 6H_2O$ (Aldrich, >98 %), $(NH_4)_2S_2O_8$ (Aldrich, > 98 %), $NaBH_4$ (Aldrich, >98 %) and glacial acetic acid (Aldrich, >99.7 %) were used as supplied without further purification. Aqueous solutions of HCl and NaOH were prepared based on the corresponding standard solutions with double distilled water.

To obtain electrocatalysts, the polymers were immobilized on a carbon substrate by means of oxidative polymerization of the corresponding monomer in acetic ($PoPDA_{HAc}$/C and $PmPDA_{HAc}$/C) or hydrochloric (only $PmPDA_{HCl}$/C) acid in the presence of dispersion of an acetylene black, followed by the introduction of cobalt, which resulted in formation of composites $PoPDA_{HAc}$-Co/C, $PmPDA_{HAc}$-Co/C and $PmPDA_{HCl}$-Co/C. This allowed to compare the spectral and electrochemical properties of the composites, which differed by either polymer type or conditions of its formation.

The synthesis of polymer-loaded carbon composites $PoPDA_{HAc}$/C and $PmPDA_{HAc}$/C was based on the previously reported method used for the synthesis of individual PoPDA [24]. Briefly, 5 g of acetylene black was dispersed in 350 ml of glacial acetic acid and then 1 g (9.25 mM) of the corresponding monomer was dissolved at 40 °C. Next, 6.38 g (28 mM) $(NH_4)_2S_2O_8$ in 10 ml of water, as an oxidant, was slowly added dropwise to the dispersion with continuous stirring, and the reaction mixture was heated under reflux (110 °C) during 54 h. The resulting precipitate of $PoPDA_{HAc}$/C or $PmPDA_{HAc}$/C composites were filtered, washed with distilled water and dried at 60 °C on air. For the synthesis of $PmPDA_{HCl}$-loaded carbon composite ($PmPDA_{HCl}$/C), the procedure, similar to preparation of individual PmPDA, was used [25]. One gram (9.25 mM) of *m*-phenylenediamine was dissolved in 40 ml of distilled water, and then 5 g of acetylene black was dispersed by ultrasonic treatment, followed by the addition of 4.99 g (18.5 mM) of $(NH_4)_2S_2O_8$ in 200 ml of 1 M HCl dropwise with continuous stirring. The reaction mixture was maintained for 24 h at room temperature (pH=1–0.5), a precipitate of composite was filtered, washed with 1 M HCl and excess of distilled water and then dried at 60 °C. Dedoping (deprotonation) of polymers in obtained polymer-loaded carbon composites $PoPDA_{HAc}$/C, $PmPDA_{HAc}$/C and $PmPDA_{HCl}$/C was carried out with excess of 0.1 M NaOH (2 h of vigorously stirring at room temperature) followed by filtration of composites, washing with excess of distilled water and drying at 60 °C on air.

For the synthesis of cobalt-containing composites, according to the procedure described in [14], the dispersions of 2 g of $PoPDA_{HAc}$/C, $PmPDA_{HAc}$/C or $PmPDA_{HCl}$/C (with dedoped polymer) in 34 ml of H_2O were placed in a three-necked flask, then a solution of 0.83 g of $Co(NO_3)_2 \times 6H_2O$ in 8 ml of water was added under stirring, the temperature was raised up to 75–80 °C and was kept under stirring for 0.5 h. Next, the reducing solution containing 1.76 g of $NaBH_4$ and 0.12 g of NaOH in 168 ml of H_2O (pH 11–12) was added dropwise under vigorously stirring to the reaction mixture. Completeness of the reduction process was controlled by pH measuring of reaction mixture. Once the pH value after a gradual reduction remained constant for 30 min, the reaction mixture was cooled to room

temperature; the precipitates of composites $PoPDA_{HAc}$-Co/C, $PmPDA_{HAc}$-Co/C or $PmPDA_{HCl}$-Co/C were filtered, washed with excess of distilled water to pH~7 and dried at 90 °C on air.

Characterization of Composites

The morphology of the obtained composites was characterized by scanning electron microscopy (JEOL F-6301) in the secondary and backscattered electrons modes. Polymer content in the composites was evaluated based on data C,H,N-analysis (Carlo Erba 1106). The automatic dual beam atomic absorption spectrometer SOLAAR S4 (Thermo Electron Co., USA) was used for determination of cobalt content in the samples. For this purpose, samples of composites were treated with conc. H_2SO_4 (80–90 °C), the mixture was transferred into a 2 % solution of HNO_3, then was filtered. The filtrate was used for determination of Co, and the precipitate to verify the completeness of cobalt dissolution by means of X-ray fluorescence (X-Supreme Spectrometer 8000, Oxford Instruments). X-ray powder diffraction patterns of the composites were measured on D8 ADVANCE diffractometer (Bruker) using filtered Cu-K_α radiation (λ=0.154 nm). FTIR spectra of polymers as components of nanocomposites were measured on FTIR SPECTRUM ONE spectrometer (Perkin Elmer) in KBr pellets.

Electrochemical Studies of Composites

Electrochemical and electrocatalytic measurements were performed in a three-electrode undivided cell (working electrode—glassy carbon disc, with an apparent surface area of 0.03 cm^2; auxiliary electrode—platinum mesh; reference electrode—Ag/AgCl (3 M KCl), E≈0.28 V vs. reversible hydrogen electrode, RHE) using computer-operated electrochemical complex based on PI-50-1 potentiostat. The potentials presented in this study are referred to the RHE. An aqueous 0.05 M H_2SO_4, saturated with either Ar or air was used as an electrolyte. Potential scan rate during cyclic voltammetry was 2 mV/s. Electrocatalyst was deposited on the electrode surface as a thin film with Nafion®. For this purpose, 2 mg of nanocomposite and 8 μl of 5 % alcoholic solution of Nafion (Aldrich) were ultrasonically dispersed in 48 ml of C_2H_5OH, then 2 μl of the obtained dispersion was dropped on the electrode surface and dried on air at room temperature.

Results and Discussion

Morphology and Composition

It is shown by scanning electron microscopy (SEM) that the morphology of the pristine carbon black (Fig. 1a) and cobalt-free composites $PoPDA_{HAc}$/C (Fig. 1b), $PmPDA_{HAc}$/C (Fig. 1e) or $PmPDA_{HCl}$/C (Fig. 1h) are similar. The small quasi-spherical grains (30–70 nm) are observed for such materials in the micrographs obtained in the secondary electron mode and there are no substantial changes of their morphology and particle size upon formation of the nanocomposites from the pristine carbon.

At the same time, for the cobalt-containing composites $PoPDA_{HAc}$-Co/C (Fig. 1c), $PmPDA_{HAc}$-Co/C (Fig. 1f) and $PmPDA_{HCl}$-Co/C (Fig. 1e) fairly large platelet-shaped particles (up to a few hundred nm) can be found on corresponding SEM images along with characteristic quasi-spherical grains. On the basis of the SEM images of the same areas of the samples but obtained in the backscattered electron mode (Fig. 1d, g, j), it can be concluded that the white plates distributed in the dark areas are associated with cobalt-containing phase.

The mass fraction of polymer in the composites was calculated based on nitrogen content in the samples (C,H,N-analysis). As can be seen from the results shown in Table 1, the weight percentage of poly(phenylenediamines) in the composites differ slightly with an equal monomer content in the reaction mixture. Moreover, the polymer content in the samples is dependent on both its chemical structure and on the polymerization conditions.

Co content in the samples varies in the range of 1 % under comparable conditions of its introduction in the composites (Table 1). And the small differences in the weight ratio of polymer to cobalt in composites (from 1:1.25 to 1:1.12) may be associated with the molecular structure of polymers that promote or hinder “entrap” of cobalt in the composite.

Infrared Spectroscopy

Unfortunately, small polymer content in the prepared composites, as well as the overlap of the characteristic bands for poly(phenylenediamines) and carbon black in their FTIR spectra did not allow to use FTIR spectroscopy in full for unambiguous interpretation of the polymer structure in such hybrid materials. Considering the above, we studied the FTIR spectra of the individual $PoPDA_{HAc}$, $PmPDA_{HAc}$ and $PmPDA_{HCl}$ synthesized by analogy with the corresponding composites assuming that their molecular structure can be close to structure of poly(phenylenediamines) as a component of composites. FTIR spectra of the $PoPDA_{HAc}$, $PmPDA_{HAc}$ and $PmPDA_{HCl}$ are given in Fig. 2.

The spectra of all poly(phenylenediamines) show two broad overlapping bands with maxima at 3300–3320 and 3215–3095 cm^{-1} (N–H stretching vibrations) that are assigned to primary and secondary amino groups present in the polymer structures, as end-groups or in open phenazine rings [26, 27]. The bands at 1613 and 1533 cm^{-1} ($PoPDA_{HAc}$) and 1620 and 1526 cm^{-1} ($PmPDA_{HAc}$ and $PmPDA_{HCl}$) are assigned to

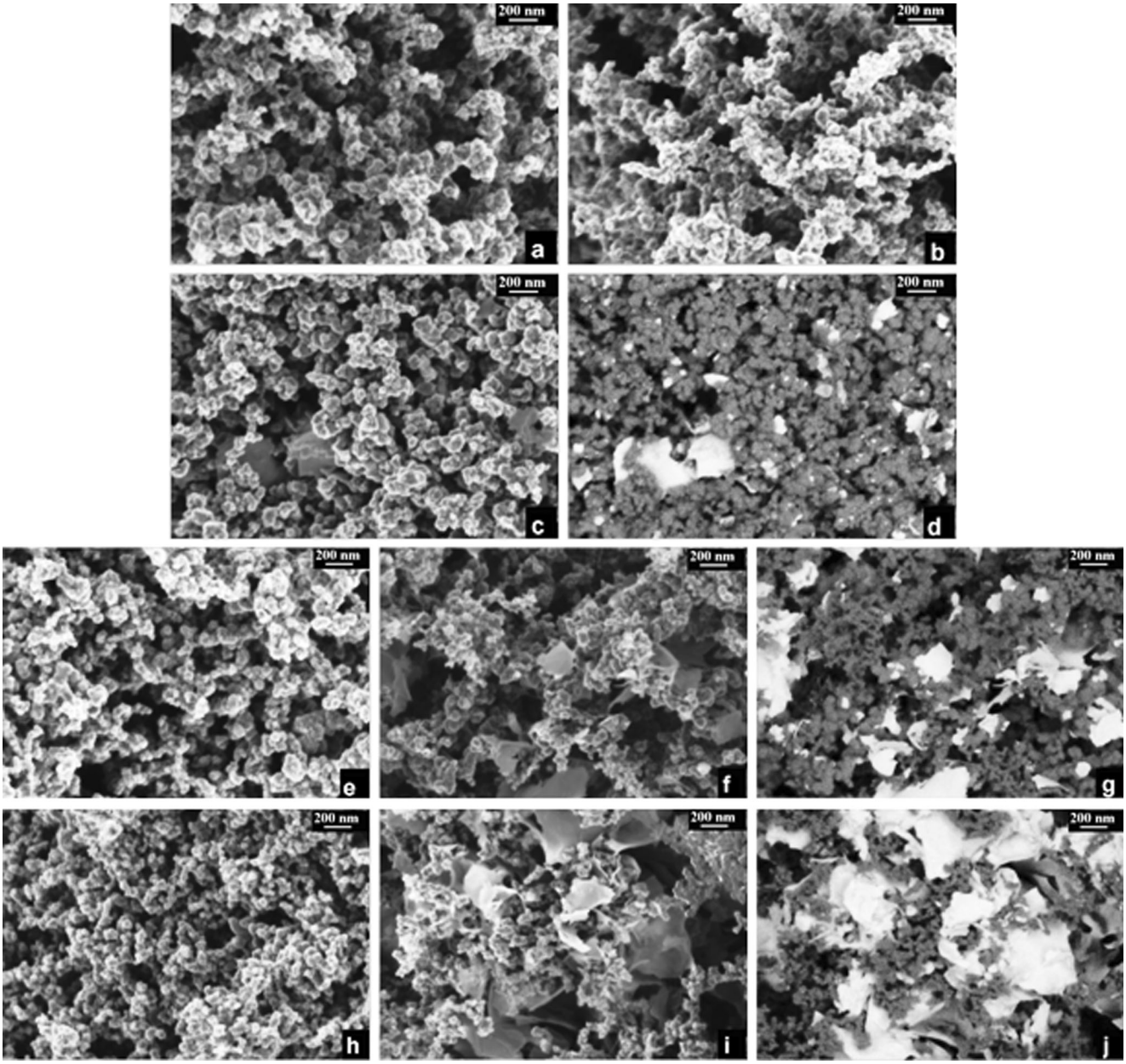

Fig. 1 SEM micrographs of pristine carbon black (**a**), composites $PoPDA_{HAc}$/C (**b**), $PmPDA_{HAc}$/C (**e**), $PmPDA_{HCl}$/C (**h**), $PoPDA_{HAc}$-Co/C (**c**, **d**), $PmPDA_{HAc}$-Co/C (**f**, **g**) and $PmPDA_{HCl}$-Co/C (**i**, **j**) in the secondary (**a**–**c**, **e**, **f**, **h**, **i**) and in the backscattered (**d**, **g**, **j**) electron modes

C═N and C═C stretching vibrations in phenazine structures, respectively [28]. The $PoPDA_{HAc}$ spectrum shows a strong peak centered at 1419 cm^{-1} that can be attributed to the ring stretching vibrations of the phenazine units in the polymer backbone [29]. The corresponding bands for $PmPDA_{HAc}$ and $PmPDA_{HCl}$ have low intensity and are shifted toward higher wavenumbers. The absorptions at 1255 and 1371 cm^{-1} ($PmPDA_{HAc}$, $PmPDA_{HCl}$) and 1211 and 1349 cm^{-1}

Table 1 C,H,N-analysis and atomic absorption spectrometry data for $PoPDA_{HAc}$-Co/C, $PmPDA_{HAc}$-Co/C and $PmPDA_{HCl}$-Co/C

Composite	C,H,N-analysis, %wt.			Polymer content, %wt. (C,H,N-analysis)	Cobalt content, %wt. (atomic absorption spectrometry)
	C	H	N		
$PmPDA_{HCl}$-Co/C	88.23	0.38	1.81	6.8	7.6
$PmPDA_{HAc}$-Co/C	88.83	0.39	1.43	5.5	6.9
$PoPDA_{HAc}$-Co/C	88.03	0.20	1.68	6.2	7.4

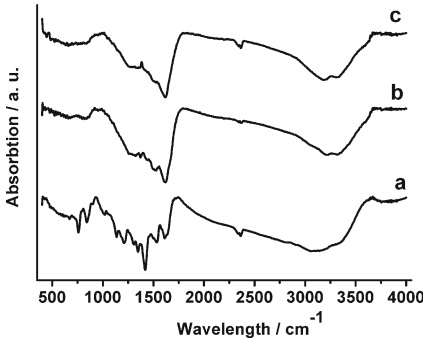

Fig. 2 FTIR-spectra of $PoPDA_{HAc}$ (**a**), $PmPDA_{HAc}$ (**b**) and и $PmPDA_{HCl}$ (**c**)

($PoPDA_{HAc}$) are assigned to C–N stretching vibrations of the quinoid and benzoid rings, respectively [30]. Another bands in $PoPDA_{HAc}$ spectrum at 1136 and 1018 cm^{-1} are ascribed to the aromatic C–H in-plane bending mode. Such bands do not appear in the $PmPDA_{HAc}$ or $PmPDA_{HCl}$ spectra.

The two fairly strong bands at 841 and 760 cm^{-1} in the spectrum of $PoPDA_{HAc}$ as well as broad and low-intensity band at 828 and 833 cm^{-1} in the spectra of $PmPDA_{HAc}$ and $PmPDA_{HCl}$, respectively, can be attributed to the out-of-plane bending vibrations of C–H bonds in 1,2,4,5-tetrasubstituted benzene nuclei of phenazine fragments [26, 31, 32]. Simultaneously, bands at 1115 and 619 cm^{-1}, assigned to in-plane and out-of-plane bending motion of the C–H bonds of the 1,2,4-trisubstituted benzene rings [33, 34], in the spectra of synthesized polymers are absent.

Thus, on the basis of the obtained results, it can be concluded about the similarity of the FTIR spectra PmPDA obtained in various ways, and some their unlike from $PoPDA_{HAc}$ spectrum. It is may be due to differences in the electronic structure of PmPDA and PoPDA as a component composites. In general, the nature of the spectra indicates the phenazine-like structure of the polymer component with the presence of free $-NH_2$ groups in such structure as a defects.

X-ray Diffraction

The X-ray diffraction (XRD) patterns of the prepared composites as well as pristine carbon black particles are shown in Fig. 3. For the pristine carbon black particles (Fig. 3a), the diffraction peaks are observed at 2θ=25.4° and 42.9° corresponding to C(002) and C(100) crystal faces [35, 36], respectively. The XRD patterns of the composites based on PmPDA (Fig. 3c, d) show peaks relating to the carbon component and the broad bands centered at 2θ=9.1; 18.6° ($PmPDA_{HAc}$-Co/C) and 9.5; 19.2° ($PmPDA_{HCl}$-Co/C) that are specific for PANI and its derivatives [36–39]. The latter indicates a predominantly amorphous state of the polymer in the composites. It should be noted that the intensive peak C(002) of the carbon substrate may overlap often observable for poly(phenylenediamines) sufficiently intense peak

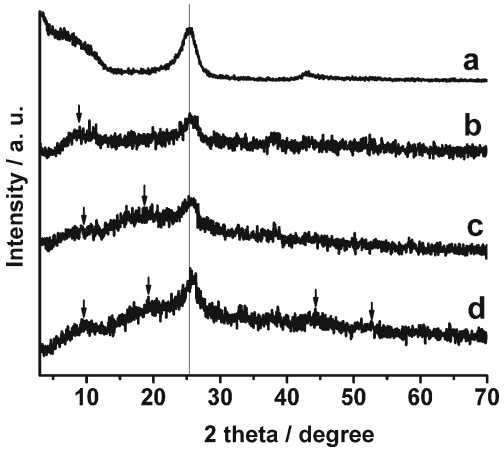

Fig. 3 XRD patterns of pristine carbon black (**a**) and composites $PoPDA_{HAc}$-Co/C (**b**), $PmPDA_{HAc}$-Co/C (**c**) and $PmPDA_{HCl}$-Co/C (**d**)

at 2θ=25°–26° [37–39]. Comparing the XRD pattern of pristine carbon black particles (Fig. 3a) with the ones of composites based on PmPDA (Fig. 3c, d), some change in the shape of the diffraction peaks in this area as well a small shift of their maxima (25.7° for $PmPDA_{HAc}$-Co/C and 26.0° for $PmPDA_{HCl}$-Co/C) can be observed, which is accordant with our assumption. Some differences in the XRD patterns of $PmPDA_{HAc}$-Co/C (Fig. 3c) and $PmPDA_{HCl}$-Co/C (Fig. 3d) most likely indicate significant similarity but not the identity of crystalline structures of composites based on PmPDA. The XRD pattern of the composite $PoPDA_{HAc}$-Co/C (Fig. 3b) is significantly different from those of analogues based on PmPDA and is characterized by the presence of two broad peaks with maxima at 2θ=8.5° and 26.0°, which indicate the dominance of amorphous structure of polymer in the composite.

As can be seen in Fig. 3d, XRD pattern of composite $PmPDA_{HCl}$-Co/C shows low-intensity peaks at 2θ=44.3° (probably overlapping with the C(100) peak of carbon component) and 52.9°, which are caused by the presence of β-Co metallic nanoparticles [40, 41]—one of the possible forms of the presence of cobalt in the composites. Interestingly enough, those similar peaks in the XRD patterns of composites $PmPDA_{HAc}$-Co/C or $PoPDA_{HAc}$-Co/C occur at a noise level or absent, despite the fact that the presence of cobalt in all composites was confirmed by atomic absorption spectrometry. The absence of obvious reflections from cobalt-containing crystalline phases in the XRD patterns can be related as to the relatively low content of this element in the composites [41], and also with a tendency of macromolecules to constrain the crystallization of Co-containing particles [42]. In accordance with [34], we can assume that cobalt in the electronic state Co^{δ} ($0 \le \delta \le 2^{+}$) is present in the composites mainly in amorphous form, including coordination with the nitrogen atoms of the polymer chain, that is not appeared in the XRD patterns.

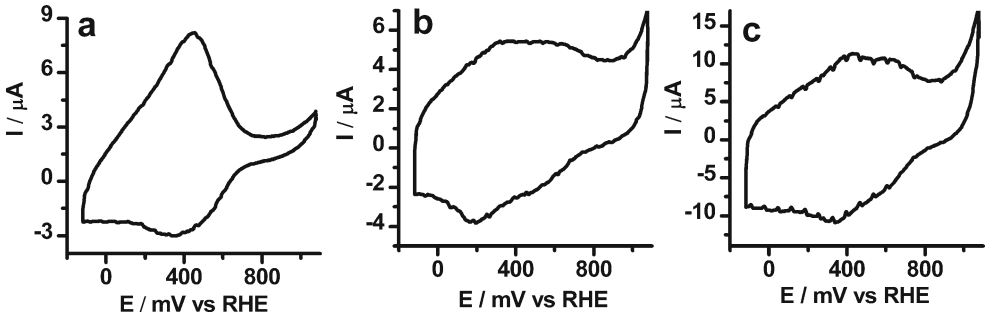

Fig. 4 Cyclic voltammograms of $PoPDA_{HAc}$-Co/C (**a**), $PmPDA_{HAc}$-Co/C (**b**) and $PmPDA_{HCl}$-Co/C (**c**) in Ar-saturated 0.05 M H_2SO_4

Electrochemical and Electrocatalytic Properties

We studied the redox properties of $PoPDA_{HAc}$-Co/C, $PmPDA_{HAc}$-Co/C and $PmPDA_{HCl}$-Co/C, as well as their ORR activity in 0.05 M H_2SO_4 to ascertain the possible effects of differences in the molecular structure of polymer component, associated with the position of the amino groups in the aromatic ring of the starting monomers, on the electrochemical characteristics of the corresponding nanocomposites.

It is shown, that the nanocomposites $PoPDA_{HAc}$-Co/C, $PmPDA_{HAc}$-Co/C and $PmPDA_{HCl}$-Co/C are electrochemically active in the range of potentials from −0.1 to 1.1 V, exhibiting a sufficiently high stability of redox characteristics during of reversible electrochemical transitions (50 cycles) in 0.05 M H_2SO_4. The presence of couple broad peaks in cyclic voltammograms (CVs) of the composites (Fig. 4) is associated with redox transitions in the corresponding amino-substituted analogue of polyaniline [31]. The broadening of the peaks and anodic shift of their maxima in CVs as compared with the

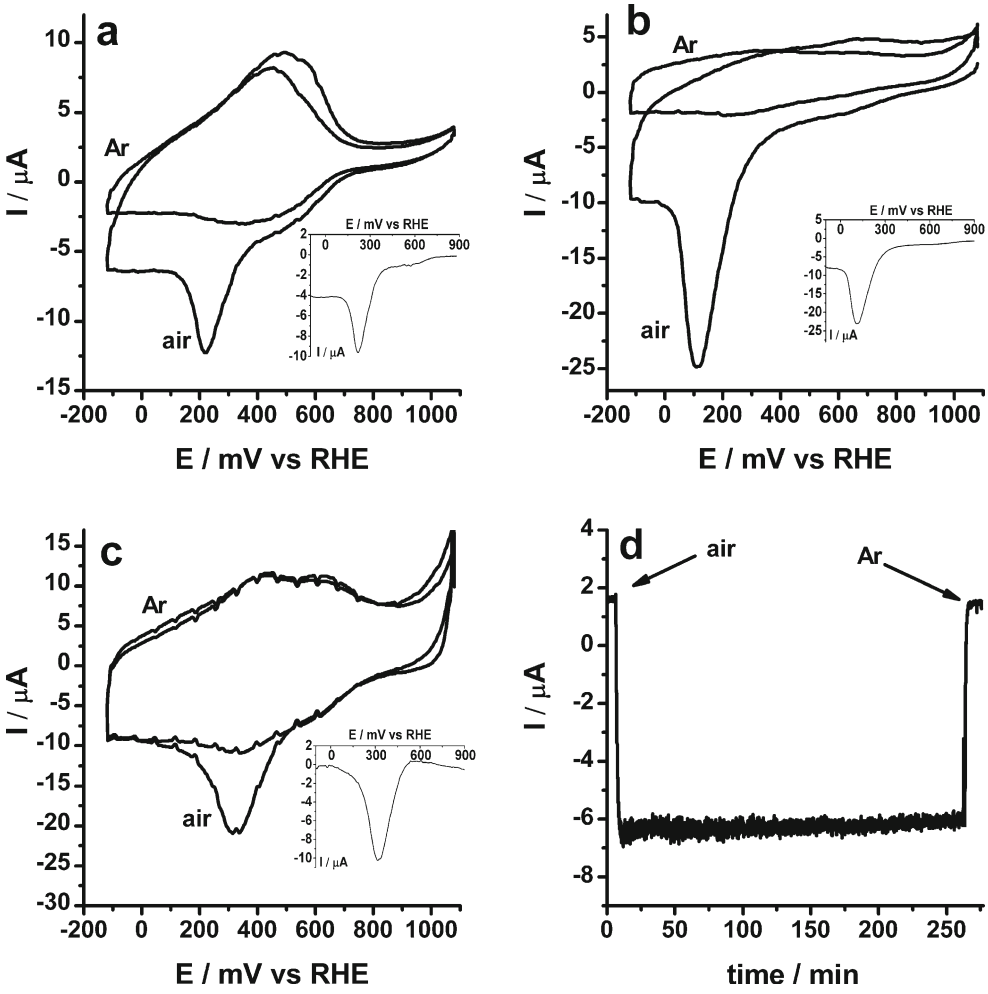

Fig. 5 Cyclic voltammograms and electrocatalytic oxygen reduction curves (*inset*) of $PoPDA_{HAc}$-Co/C (**a**), $PmPDA_{HAc}$-Co/C (**b**) and $PmPDA_{HCl}$-Co/C (**c**) in 0.05 M H_2SO_4. Chronoamperometric response of $PmPDA_{HCl}$-Co/C at 180 mV in air-saturated 0.05 M H_2SO_4 (**d**)

individual PmPDA and PoPDA may be due to hindered electron transfer in the composites.

We have studied redox properties of the obtained nanocomposites in air-saturated 0.05 M H_2SO_4 in order to clarify their ability to exhibit electrocatalytic properties in ORR. The activity of these nanocomposite electrocatalysts was characterized by electrocatalytic oxygen reduction curves, representing the difference between the cathodic branches of CVs recorded in the presence of air and deaerated conditions. The appearance of irreversible wave at the cathode branch of CVs in air-saturated electrolyte (Fig. 5) indicates activity of composites in ORR, and the content of the polymer and cobalt in composites as well as the type of polymer or the method of its preparation have influence on the functional characteristics of these electrocatalysts at that. One should point out that electrocatalytic activity in ORR of the bare GC electrode is low under the measurement conditions, and the main contribution into the current-producing process is provided by electrochemical oxygen reduction on nanocomposite electrocatalysts.

It is interesting to note, that growth of polymer and cobalt contents in the composite electrocatalysts (Table 1) lead to anodic shift of ORR peak potential (E_p) regardless of the type of polymer and method of its preparation (Fig. 5). At the same time, a clear correlation between mass fraction of the polymer or cobalt in electrocatalysts and ORR onset potential (E_{onset}) or catalytic currents is not observed. So $PoPDA_{HAc}$-Co/C, as ORR electrocatalyst, is characterized by E_{onset}~430 mV and maximum of catalytic current at 220 mV (Fig. 5a). The $PmPDA_{HAc}$-Co/C nanocomposite obtained under the same conditions shows the E_{onset} value practically unchanged as compared with $PoPDA_{HAc}$-Co/C, but there is a growth of the catalytic current and significant cathodic shift of E_p up to ~115 mV (Fig. 5b). The $PmPDA_{HCl}$-Co/C composite based on the same polymer but obtained by using hydrochloric acid shows the highest E_p~ 325 mV and E_{onset}~530 mV among all the prepared ternary nanocomposite electrocatalysts (Fig. 5c), while the catalytic current is close to the value for $PoPDA_{HAc}$-Co/C (Fig. 5a).

In our opinion, observed features of the electrochemical properties of nanocomposites can be related to differences in the structure of the polymer components, which cause not only differ in ability of poly(phenylenediamines) "to entrap" cobalt into composite during formation, but also the differences in the cobalt environment in C/CoN_x or CoN_x sites of electrocatalyst, on which adsorption, activation and catalytic conversion of O_2 are provided [2, 5, 18, 36, 42], i.e. to affect the amount of catalytically active sites and their effectiveness.

The stability of electrocatalysts activity in the course of their functioning is an important characteristic. Figure 5d shows the chronoamperometric response of the GC electrode, modified with $PmPDA_{HCl}$-Co/C composite at a constant potential 180 mV. It is evident from Fig. 5d that the introduction of air into the electrochemical cell results in appearance of electrocatalytic current, reaching rather fast the steady state and featuring no significant decrease in time. The decrease in ORR activity was found to be less than 5 % for $PmPDA_{HCl}$-Co/C-based electrode at the end of 4 h. This clearly demonstrated a rather high stability of ORR activity of $PmPDA_{HCl}$-Co/C electrocatalyst in acidic electrolyte.

It was of interest to ascertain the effect of the individual components of composites on the ORR activity and their

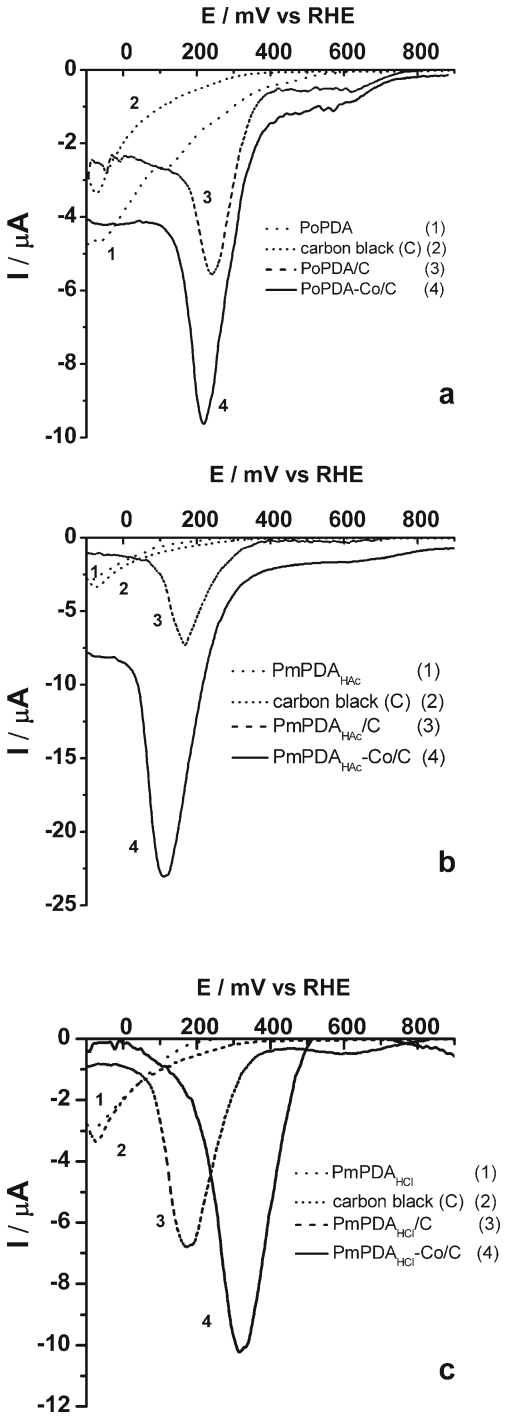

Fig. 6 Electrocatalytic oxygen reduction curves for composites $PoPDA_{HAc}$-Co/C (**a**), $PmPDA_{HAc}$-Co/C (**b**) and $PmPDA_{HCl}$-Co/C (**c**) and their individual components in 0.05 M H_2SO_4

contribution to the reduction of oxygen. It is found (Fig. 6), that the carbon black and individual polymer, regardless of its structure and method of preparation, exhibit low activity in ORR. At the same time, cobalt-free composites $PoPDA_{HAc}$/C, $PmPDA_{HAc}$/C and $PmPDA_{HCl}$/C have markedly better characteristics but E_{onset} and catalytic currents for such composites in ORR are lower than for the corresponding cobalt containing analogues. Moreover, for nanocomposite $PmPDA_{HCl}$-Co/C, along with an increase of E_{onset} and catalytic current, E_p anodic shift more than on 140 mV takes place.

It should be noted that the activity of $PoPDA_{HAc}$-Co/C, $PmPDA_{HAc}$-Co/C and specially $PmPDA_{HCl}$-Co/C are markedly higher than that for previously reported similar PANI-based composite (E_{onset}~420 mV; E_p~−10 mV vs. RHE) [20], which may be due to effective formation and/or increase the number of C/CoN_x or CoN_x sites in electrocatalysts at the expense of the presence of additional nitrogen atoms in poly(phenylenediamines).

Conclusion

In conclusion, we obtained ternary metal-polymer nanocomposites based on amino-substituted analogues of polyaniline (PoPDA, PmPDA), cobalt and carbon black—$PoPDA_{HAc}$-Co/C, $PmPDA_{HAc}$-Co/C and $PmPDA_{HCl}$-Co/C, which are capable of exhibiting sufficiently high activity for the ORR (E_{onset} 430–530 mV; E_p 115–325 mV vs. RHE). It is shown that differences in the structure of PoPDA and PmPDA due to the position of the amino groups in the aromatic ring of the starting monomers, as well as conditions for their preparation, cause the difference in the electrochemical properties of hybrid composites based on such polymers. It is found that nanocomposite electrocatalysts based on PmPDA, compared with the composite based on PoPDA, are characterized by either more positive E_{onset} and E_p values ($PmPDA_{HCl}$-Co/C) or greater catalytic currents ($PmPDA_{HAc}$-Co/C) in 0.05 M H_2SO_4. It is shown that the ORR activity of cobalt containing composites based on poly(phenylenediamines) exceed those, previously set, for analogue based on polyaniline.

Acknowledgments The work was partly financially supported by the Target Complex Program of Scientific Research of National Academy of Sciences of Ukraine "Hydrogen in renewable energy and new technologies" (project no. 6) and Ukrainian State Target Scientific and Technical Program "Nanotechnologies and Nanomaterials" (project no. 6.22.3.11).

References

1. C. Sealy, Mater. Today **11**, 65 (2008)
2. F. Jaouen, E. Proietti, M. Lefevre, R. Chenitz, J.-P. Dodelet, G. Wu, H.T. Chung, C.M. Johnston, P. Zelenay, Energy Environ. Sci. **4**, 114 (2011)
3. J.P. Dodelet, in *N4-macrocyclic metal complexes*, ed. by J.H. Zagal, F. Bedioui, J.P. Dodelet (Springer Science + Business Media Inc., New-York, 2006)
4. Z. Chen, D. Higgins, A. Yu, L. Zhang, J. Zhang, Energy Environ. Sci. **4**, 3167 (2011)
5. C.W.B. Bezerra, L. Zhang, K. Lee, H. Liu, A.L.B. Marques, E.P. Marques, H. Wang, J. Zhang, Electrochim. Acta **53**, 4937 (2008)
6. A. Garsuch, A. Bonakdarpour, G. Liu, R. Yang, J. R. Dahn, in *Handbook of fuel cells: advances in electrocatalysis, materials, diagnostics and durability, vol. 5 & 6*, ed. by W. Vielstich, H.A. Gasteiger, H. Yokokawa (John Wiley & Sons, Ltd., 2009)
7. D. Geng, H. Liu, Y. Chen, R. Li, X. Sun, S. Ye, S. Knights, J. Power Sources **196**, 1795 (2011)
8. K. Parvez, S. Yang, Y. Hernandez, A. Winter, A. Turchanin, X. Feng, K. Müllen, ACS Nano **6**, 9541 (2012)
9. V.G. Khomenko, V.Z. Barsukov, A.S. Katashinskii, Electrochim. Acta **50**, 1675 (2005)
10. M. Hasik, A. Pron, I. Kulszewicz-Bajer, A. Pozniaczek, A. Bielanski, Z. Piwowarska, R. Dziembaj, Synth. Met. **55–57**, 972 (1993)
11. Z. Qi, P.G. Pickup, Chem Commun, 2299 (1998)
12. Y.I. Kurys, O.S. Dodon, O.O. Ustavytska, V.G. Koshechko, V.D. Pokhodenko, Russ. J. Electrochem. **48**, 1058 (2012)
13. K. Lee, L. Zhang, H. Lui, R. Hui, Z. Shi, J. Zhang, Electrochim. Acta **54**, 4704 (2009)
14. G. Wu, K.L. More, C.M. Johnston, P. Zelenay, Science **332**, 443 (2011)
15. M. Lefevre, E. Proietti, F. Jaouen, J.P. Dodelet, Science **324**, 71 (2009)
16. G. Wu, M.A. Nelson, N.H. Mack, S.G. Ma, P. Sekhar, F.H. Garzon, P. Zelenay, Chem. Commun. **46**, 7489 (2010)
17. G. Wu, N.H. Mack, W. Gao, S. Ma, R. Zhong, J. Han, J.K. Baldwin, P. Zelenay, ACS Nano **6**, 9764 (2012)
18. C. M. Johnston, P. Piela, P. Zelenay, in *Handbook of Fuel cells: advances in electrocatalysis, materials, diagnostics and durability, volumes 5 & 6*, ed. by W. Vielstich, H.A. Gasteiger, H. Yokokawa (John Wiley & Sons, Ltd., 2009)
19. R. Bashyam, P. Zelenay, Nat. Lett. **443**, 63 (2006)
20. W.M. Millan, T.T. Thompson, L.G. Arriaga, M.A. Smit, Int. J. Hydrog. Energy **34**, 694 (2009)
21. T. Hirayama, T. Manako, H. Imai, e-J. Surf. Sci. Nanotechnol. **6**, 237 (2008)
22. M. Yuasa, A. Yamaguchi, H. Itsuki, K. Tanaka, M. Yamamoto, K. Oyaizu, Chem. Mater. **17**, 4278 (2005)
23. K. Asazawa, K. Yamada, H. Tanaka, A. Oka, M. Taniguchi, T. Kobayashi, Angew. Chem. Int. Ed. **46**, 8024 (2007)
24. P. Wang, Z. Ma, Z. Zhao, L. Jia, J. Electroanal. Chem. **611**, 87 (2007)
25. H.S.O. Chan, S.C. Ng, T.S.A. Hor, J. Sun, K.L. Tan, B.T.G. Tan, Eur. Polym. J. **27**, 1303 (1991)
26. A.H. Premasiri, W.B. Euler, Macromol. Chem. Phys. **196**, 3655 (1995)
27. M.R. Huang, X.G. Li, Y. Yang, Polym. Degrad. Stab. **71**, 31 (2001)
28. Q. Hao, B. Sun, X. Yang, L. Lu, X. Wang, Mater. Lett. **63**, 334 (2009)
29. T.J. Durnick, S.C. Wait, J. Mol. Spectrosc. **42**, 211 (1972)
30. D. He, Y. Wu, B.Q. Xu, Eur. Polym. J. **43**, 3703 (2007)
31. X.-G. Li, M.-R. Huang, W. Duan, Chem. Rev. **102**, 2925 (2002)
32. R.H. Sestrem, D.C. Ferreira, R. Landers, M.L.A. Temperini, G.M. do Nascimento, Polymer **50**, 6043 (2009)
33. J. Han, J. Dai, R. Guo, J. Colloid Interface Sci. **356**, 749 (2011)
34. M.-R. Huang, Q.-Y. Peng, X.-G. Li, Chem. Eur. J. **12**, 4341 (2006)
35. B. Manoj, A.G. Kunjomana, Int. J. Electrochem. Sci. **7**, 3127 (2012)
36. G. Wu, Z. Chen, K. Artyushkova, F.H. Garzon, P. Zelenay, ECS Trans. **16**, 159 (2008)

37. C. Zhou, Z. Liu, X. Du, D.R.G. Mitchell, Y.-W. Mai, Y. Yan, Nanoscale Res. Lett. **7**, 165 (2012)
38. T. Li, C. Yuan, Y. Zhao, Q. Chen, M. Wei, Y. Wang, J. Macromol. Sci. A **50**, 330 (2013)
39. J.P. Pouget, M.E. Jozefowicz, A.J. Epstein, X. Tang, A.G. MacDiarmid, Macromolecules **24**, 779 (1991)
40. C. Walter, K. Kummer, D. Vyalikh, V. Brüser, A. Quade, K.-D. Weltmann, J. Electrochem. Soc. **159**, F494 (2012)
41. D. Nguyen-Thanh, A.I. Frenkel, J. Wang, S. O'Brien, D.L. Akins, Appl. Catal. B **105**, 50 (2011)
42. J. Wang, H. Qin, J. Liu, Z. Li, H. Wang, K. Yang, A. Li, Y. He, X. Yu, J. Phys. Chem. C **116**, 20225 (2012)